Landslides (2015) 12:997–1005
DOI 10.1007/s10346-015-0610-5
Received: 10 March 2015
Accepted: 7 July 2015
Published online: 28 July 2015

Ben Leshchinsky · Farshid Vahedifard · Ho-Bon Koo · Seung-Hyun Kim

Yumokjeong Landslide: an investigation of progressive failure of a hillslope using the finite element method

Abstract The presented case study describes the progressive movement of a shallow landslide in Central South Korea after excavation of its toe and subsequent, sustained above-average rainfall. Measured soil data as well as real-time measurements of slope movement and precipitation enabled calibration of a numerical model based on the finite element method (FEM) to capture the destabilization and associated movement of the slope. The numerical model employed the Bishop's effective stress approach to define the state of stresses in unsaturated soils, as well as transient seepage analyses to introduce the non-uniform effects of actual rainfall data into the analysis. The resulting model provided insight into the complex behavior of a progressively failing slope. It demonstrates that use of numerical methods like FEM that allow for coupled transient unsaturated seepage-stress analyses presents a means of evaluating the progressive failure of slopes under rainfall. Furthermore, it demonstrated that for certain slopes under partially saturated conditions, sustained above-average rainfall may cause shallow landsliding when driven by stimuli like excavation. Additionally, the kinematics of failing slopes may not always follow classical slope stability approaches (sliding block method, circular method of slices, log-spiral, etc.) prior and during slope failure. The given kinematics of a slope failure may change with movement, redistribution of principal stresses, and dissipation of suction stress. Therefore, analyses like FEM present a unique tool to evaluate the deformation behavior of failing slopes on a case-by-case basis.

Keywords Landslide · Partial saturation · Rainfall · Transient seepage · Finite element method · ABAQUS · Progressive slope instability

Introduction

Landslides are natural hazards that have devastating economic and social costs, sometimes with tragic impacts, including loss of human life. These slope failures, ubiquitous in both the natural and engineered slopes and earthen structures, are often associated with destabilizing events such as excavation, erosion, seismic activity, or heavy and/or sustained precipitation. For unsaturated soils, variations in suction stress due to changes in soil moisture often govern the mechanical behavior in natural and man-made slopes. The effects of negative pore water pressures and associated loss of suction due to rainfall infiltration on slope failures have long been an area of interest, prompting several investigations on the behavior of soil under unsaturated flow conditions (e.g., Lu and Likos 2004; Godt et al. 2009; Ling et al. 2009; Ling and Ling 2012; Vahedifard et al. 2014; Iverson et al. 2015). Built within many of these studies is the premise that many natural slopes are only marginally stable and prone to landsliding when capillary forces disappear due to above normal groundwater infiltration and changes in hydrological schemes (Pagano et al. 2010; Tsai et al. 2008; Leung and Ng 2013; Wang et al. 2014). Such conclusions are extremely important in context of progressive slope failures that occur during significant precipitation events.

In addition to the role of matric suction, proper consideration of failure kinematics is a critical factor in analyzing any slope. There are several approaches to evaluating slope stability, often based on soil strength properties, slope geometry, geologic conditions, water table, and assumed failure kinematics, most of which neglect any estimate of soil displacement. Depending on the soil type and the bedrock conditions, kinematics may have a major effect on the type of landslide that is realized and the most effective means of evaluating stability. For example, deep-seated landslides in clayey materials may encounter rotational failures, best accounted for using limit equilibrium (LE) methods employing log-spiral or circular arc mechanisms (Mencl 1966; Leshchinsky 1995; Vahedifard et al. 2014, 2015a, b). However, many slides occur in shallow, weathered materials overlying bedrock, often manifesting as a "plate" failure or infinite slope failure. Such a stability analysis may be performed by evaluating the equilibrium of forces on a single, representative slice of the sliding slope. Such an analysis may account for water table and unsaturated soil conditions (Lu and Godt 2008), but the latter may be difficult to evaluate using conventional LE or limit analysis methods as a coupled seepage analysis is required, kinematics must be assumed, and no information about progressive slope deformation is provided (Leshchinsky 2013; Leshchinsky and Ambauen 2015). However, use of complex finite element (FE) analyses employing coupled stress-seepage analyses, including unsaturated soil behavior and plasticity, provides an excellent framework for not only evaluating slope stability but simulating progressive movement of slopes under heavy and/or prolonged precipitation. Coupled FE analyses involving unsaturated soils have been performed, often with the intention of observing the change in soil stability under precipitation events (Yoo and Jung 2006; Lu et al. 2012). However, less literature exists with regards to progressive slope movement under real, transient seepage conditions stemming from precipitation.

This study describes the progressive movement of a shallow landslide in Central South Korea after excavation of its toe and subsequent, sustained above-average rainfall. Presented within this case study is a comparison of the measured values versus those obtained from a coupled unsaturated transient seepage-stress FE modeling.

Effective stress in variably saturated soils

In order to capture the coupled behavior of the slopes under partially saturated seepage, basic principles of unsaturated soil mechanics were required. Matric suction, the attraction between partially saturated grains of soil due to water's surface tension, may significantly influence effective shear strength for partially saturated soils. In the current study, the effects of suction on soil shear strength were quantified by incorporating the suction stress-

based effective stress representation (e.g., Bishop effective stress 1959) into the FE modeling.

The effective stress approach proposed by Bishop (1959) presents on approach that can be used in conjunction with Mohr-Coulomb failure criterion to determine the shear strength of unsaturated soils as follows:

$$\tau = c' + [(\sigma - u_a) + \chi(u_a - u_w)]\tan\phi' \quad (1)$$

where τ is shear stress, c' is effective cohesion, σ is total stress, u_a is air pressure, χ is Bishop's effective stress parameter, u_w is pore ware pressure, ϕ' is effective internal angle of friction, and the difference $(\sigma - u_a)$ is the net normal stress. Within this analysis, χ was set to the effective degree of saturation, S_e, to properly account for variation of effective stress versus saturation. The effective degree of saturation can be expressed as

$$S_e = \frac{S - S_r}{1 - S_r} \quad (2)$$

where S is the pore water degree of saturation and S_r is the residual saturation. Residual saturation is a relatively small value and refers to water content due to soil particle hydration. It can be measured or identified by the soil water characteristic curve (SWCC). For example, residual saturation of sand is 0~0.03 (e.g., Lu and Likos 2004). The saturation at each step was updated based on the soil's water retention characteristics represented by the SWCC. Moreover, SWCC as well as hydraulic conductivity function (HCF) are needed in the coupled stress-pore pressure formulation that requires to model unsaturated flow under a transient flow condition. SWCC and HCF were defined using van Genuchten (1980)–Mualem (1976)'s approach. The SWCC is defined as (e.g., Lu and Likos 2004, 2006)

$$S_e = \left[\frac{1}{1 + [\alpha(u_a - u_w)]^n}\right]^{1-1/n} \quad (3)$$

With a respective HCF defined by Gardner (1958):

$$k = k_s e^{-\alpha(u_a - u_w)} \quad (4)$$

Both the SWCC and HCF, dependent on S_e and fitting parameters α and n, can be implemented into a coupled formulation within a finite element analysis (e.g., Yoo 2013, 2014). When using FE to model a coupled pore pressure-stress formulation, the soil is treated as a porous medium in a solid phase (i.e., no action colloidal or liquid phases), discretized by a mesh used to evaluate equilibrium for prescribed increments of time. Implementation of stress-pore pressure coupled equilibrium formulation is described by Yoo (2013), where equilibrium is based on the principle of virtual work, defined as

$$\int_V \boldsymbol{\sigma} : \delta\varepsilon dV = \int_S \boldsymbol{t}\cdot\delta\boldsymbol{v}\ dS + \int_V \boldsymbol{f}\cdot\delta\boldsymbol{v}\ dV + \int_V (Sn + n_t)\rho_w \boldsymbol{g}\cdot\delta\boldsymbol{v}\ dV \quad (5)$$

where V is volume, $\boldsymbol{\sigma}$ is the true stress, $\delta\varepsilon$ is the virtual rate of deformation, $\delta\boldsymbol{v}$ is the virtual velocity, $\boldsymbol{t}$ is surface tractions per unit area, $\boldsymbol{f}$ are all body forces except the weight of the wetting liquid (water), n is the porosity, n_t is the trapped, static volume of water per unit volume of the porous media, ρ_w is the mass density of water, and g is gravity (Yoo 2013; Hibbitt et al. 2001). The integral of the last term in Eq. (5) represents the body forces of both trapped water in the voids (n_t) and the volumetric flow rate of water (effective velocity) to capture both the weight of the water and the inertial effects of flow, known as the Forchheimer term (Hibbitt et al. 2001). The principle of virtual work presented in Eq. (5) is evaluated for equilibrium in the discretized mesh volume for each respective time increment under transient seepage induced by boundary conditions representative of rainfall.

Yumokjeong Landslide

Potential effects of a changing climate include increased intensity of extreme precipitation, as has been documented in the Korean Peninsula within recent years (e.g., Yoo 2014). Similarly, annual rain and rain intensity have significantly increased in this region within the past few decades (Yoo 2014). These climate trends have noticeably increased the number of catastrophic disasters such as typhoons and precipitation-induced landslides in this region. Due to these disasters, over 1300 people were killed, 280,000 people were displaced and over 2 billion dollars in damages have been reported in South Korea from 1993 to 2012 (Yoo 2014). Among others, precipitation-induced landslides have been the major cause for casualties and economic loss. Severe rainfall events result in substantial and unprecedented changes in the degree of saturation within the unsaturated zone of man-made or natural slopes, which can lead to failure of these slopes. Occurrence of many precipitation-induced landslides in unsaturated soils highlights the need for explicit consideration of the negative pore pressure or matric suction above the water table in modeling and monitoring of theses slopes.

Lying within the central Mountainous region of South Korea, approximately 100 km east of Seoul, an excavation of a road cut and subsequent years of above-average rainfall triggered the progressive movement of a shallow, translational slide. The slope located at coordinates N (37° 35′ 20.8″), E (127° 45′ 34.4″) (terrain model shown in Fig. 1) was instrumented with wire tension meters for post-construction quality control (Fig. 2), along with a series wire tension meters on adjacent slopes. These instruments, which transmitted data wirelessly, collected slope movement data at once per day.

The slope consisted of a shallow soil layer (5–8.5 m deep) of lightly cemented, colluvial soil classified as well-graded sand (SW) overlying weathered bedrock (Fig. 3). A trace presence of fines (clay) contributed to light cementation. Based on laboratory testing, the soil's saturated hydraulic conductivity was measured to be 5E-5 m/s with a strength of ϕ'=20° and c'=15 kPa attained from a direct shear apparatus. Saturated hydraulic conductivity was found to be 5E-5 m/s for the weathered soil. Precipitation was measured at a weather station near the construction site. Beginning at the date of excavation (August 2007), progressive displacement occurred (Fig. 4a) with above-average rainfall (Fig. 4b). Over a period of 5 years, almost 350 mm of movement occurred at the measured displacement monitoring point, with a total measured rainfall of approximately 8000 mm. Visible erosion along the slope was noted after subsequent rainy seasons, likely due to extremely heavy rainfall and saturated soil conditions. This progressive slope failure was colloquially known as the "Yumokjeong" landslide based on its location.

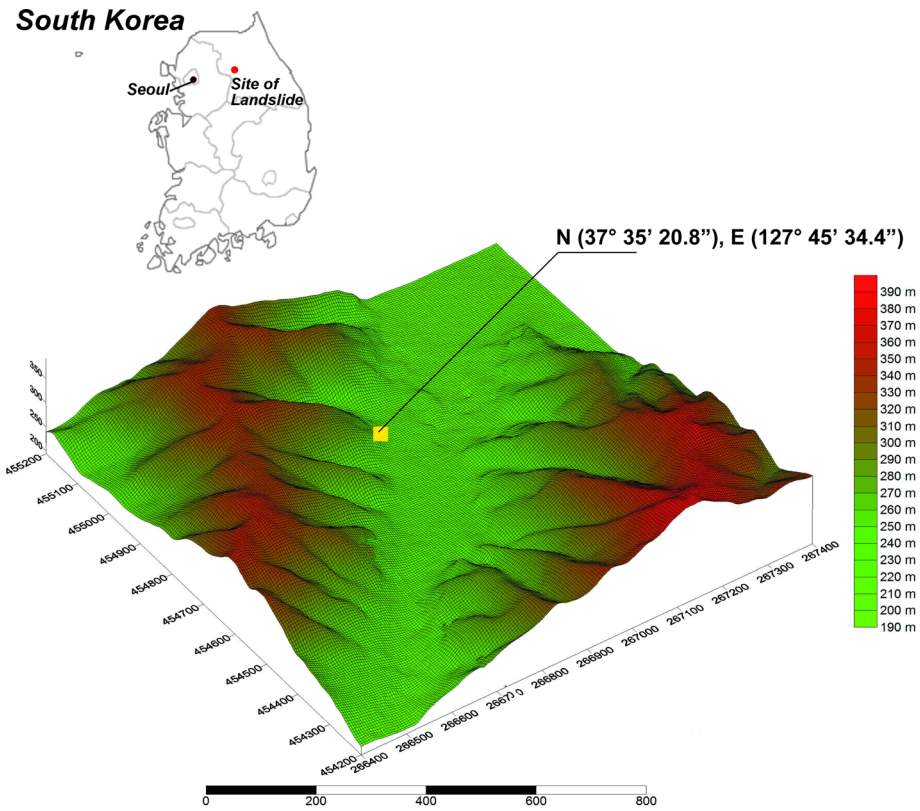

Fig. 1 Location of slope failure along highway corridor—center of topographical map, coordinates N (37° 35′ 20.8″), E (127° 45′ 34.4″).

Numerical simulation of unsaturated seepage-stress coupling

A FE analysis was performed to capture coupled behavior of the slope under transient, unsaturated seepage conditions. When using FE to model a coupled pore pressure-stress formulation, the soil is treated as a porous medium in a solid phase (i.e., no action as a colloid or liquid). To implement this coupled formulation, the SWCC as well as HCF were directly implemented (Fig. 5) into Abaqus Version 12 (Hibbitt et al. 2001), as has been done in previous studies (e.g., Yoo 2013, 2014). The implementation of these properties enabled application of Bishop's (1959) model for applying matric suction directly within the framework of Mohr-Coulomb failure criteria. The SWCC was implemented into Abaqus by adding *sorption* material properties to the soil, implementing a range of saturation values and associated suction stress values, $(u_a - u_w)$ representative of the SWCC fitted to the n and α parameters necessitated by the van Genuchten (1980)-Mualem (1976) approach. The hydraulic conductivity was assigned as a function of the degree of saturation, implemented to represent the HCF from Gardner (1958), also dependent on the α parameter.

To perform the stress-pore pressure-displacement analysis, a mesh consisting of 2259 eight-node pore-stress, reduced-integration quadrilateral elements (CPE8RP) was used to discretize the rock and the soil materials (Fig. 6). A more refined mesh was used to model the soil layer due to higher expected movement and plastic behavior, comprised of 677 elements. The remaining 1582 elements were used to mesh the rock, which was treated as an elastic material due to its competence in comparison to the overlying soil. Although weathered rock may demonstrate plastic behavior, the relative strength of the overlying colluvium was considered notably weaker, manifested by the demonstrated, progressive slope failure. The weathered rock was modeled with the same permeability as the soil as its weathered and fractured nature lends itself to a higher permeability due to the presence of fractures, fissures and macropores (George 1992; Terzaghi et al. 1996; Hsieh 1998; Jiao et al. 2005). It is difficult to capture this phenomenon discretely with continuum methods like FEM, but the higher permeability was homogenized throughout the rock elements to simplify computations. The model geometry was modeled with basic soil properties representative of Mohr-Coulomb plasticity, coupled with potential matric suction resulting from partial saturation from the transient seepage analysis. As was established from laboratory direct shear testing, approximate strength values of $\phi' = 20°$ and $c' = 15$ kPa were used to define Mohr-Coulomb criteria. The initial degree of saturation was represented as 0.45 as to represent conditions determined in laboratory testing when the excavation was

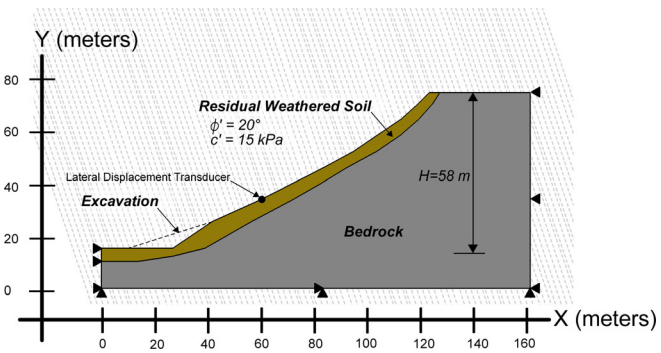

Fig. 2 Site schematic and soil properties

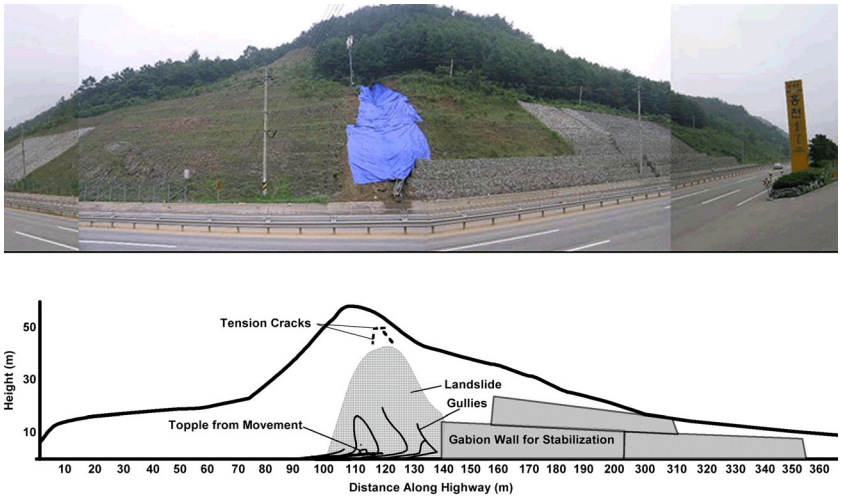

Fig. 3 Yumokjeong slope failure

performed. Initial conditions can have a significant effect on the analysis and were brought to a steady state by assigning inward seepage flux boundary conditions equivalent to the allowable permeability for a period of 30 days prior to the analysis. The importance of establishing initial boundary conditions for hydrological purposes has been emphasized by Yoo (2013). In this case, limited information was present to establish the hydrological scheme of the slope; therefore, an initial uniform value was chosen as the construction was performed in dry summer months. The material properties are presented in Table 1 and

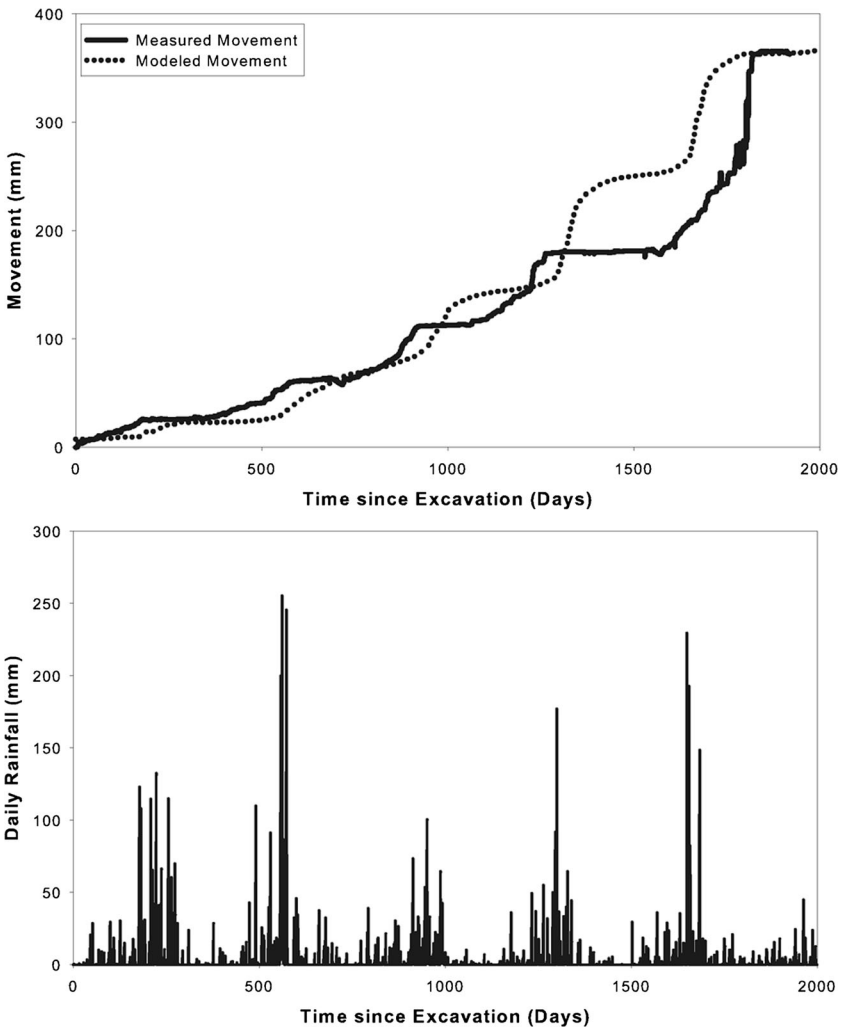

Fig. 4 **a** Slope movement and cumulative rainfall after excavation of toe. **b** Daily measured rainfall totals for site

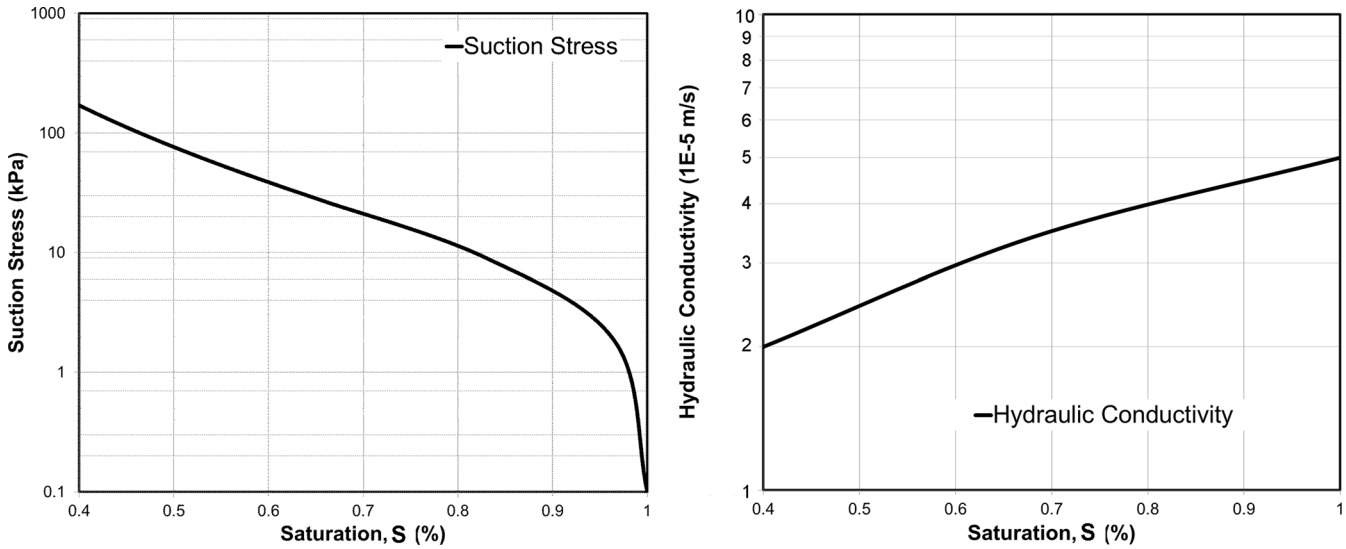

Fig. 5 **a** Matching soil water characteristic curve (SWCC). **b** Hydraulic conductivity function

are based on properties from a similar soil-type modeled by Yoo (2013, 2014).

Infiltration was modeled as a boundary condition along the top edges of the slope and was directly inferred from actual rainfall data. The infiltration rate, q, was defined as the daily average rainfall (Fig. 7a) and was limited by the saturated hydraulic conductivity of the soil per unit of slope surface area normal to the horizontal plane. That is, for large rainfall events, excess precipitation was truncated from the infiltration rate as it was assumed to flow off the surface due to exceeding hillslope permeability. This observation is supported by notable erosion and rill formation along the hillslope due to sheet and channel flow after very large storm events. Seepage out of the system was enabled by assigning seepage boundary conditions equivalent to the saturated flow rate at the excavated face, right of way and left soil boundary. The infiltration curve versus the cumulative rainfall (mm) is presented in Fig. 7a. Other factors that may affect infiltration but were not considered include vegetation and canopy cover, development of tension cracks, rainfall velocity, angle of rainfall, soil inhomogeneity, and soil anisotropy.

Results and comparison

Progressive failure of the slope was modeled by comparing field measurements of horizontal displacement to recorded horizontal displacements within the finite element mesh, demonstrating reasonable agreement. This comparison was made based on measurements from a transducer placed on the slope, 20 m vertical of the right of way. A commensurate node was selected for comparison within the finite element analysis. The comparison of slope movement, presented in Fig. 7a, demonstrates agreement between the progressive movements of the slope. A comparison of rainfall departure (the difference between measured cumulative precipitation and average cumulative precipitation) suggests that sustained, above-average, rainfall could have induced a progressive failure of the slope (Fig. 7b). For this particular scenario, the magnitude of precipitation events may have been less critical to destabilizing the slope than sustained above-average precipitation over the region's rainy season, catalyzed by excavation of the toe of the slope for highway construction. It is known that toe resistance can significantly contribute to the stability of slopes and earth structures, and excavation or erosion of the toe will play a destabilizing role (e.g., Leshchinsky and Vahedifard 2012). The

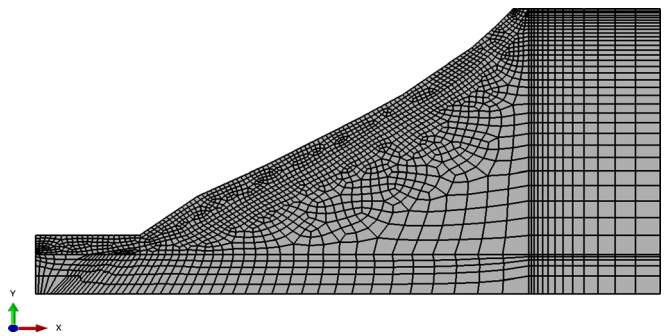

Fig. 6 Mesh used in transient seepage/stress analysis

Table 1 Material properties used in FE analysis

	Soil	Rock
γ (kN/m^3)	1400	1850
φ' (°)	20	–
c' (kPa)	15	–
E (MPa)	30	100
ν	0.3	0.3
k_{sat} (m/s)	5E-5	5E-5
α (m^{-1})	0.2	–
n	1.2	–

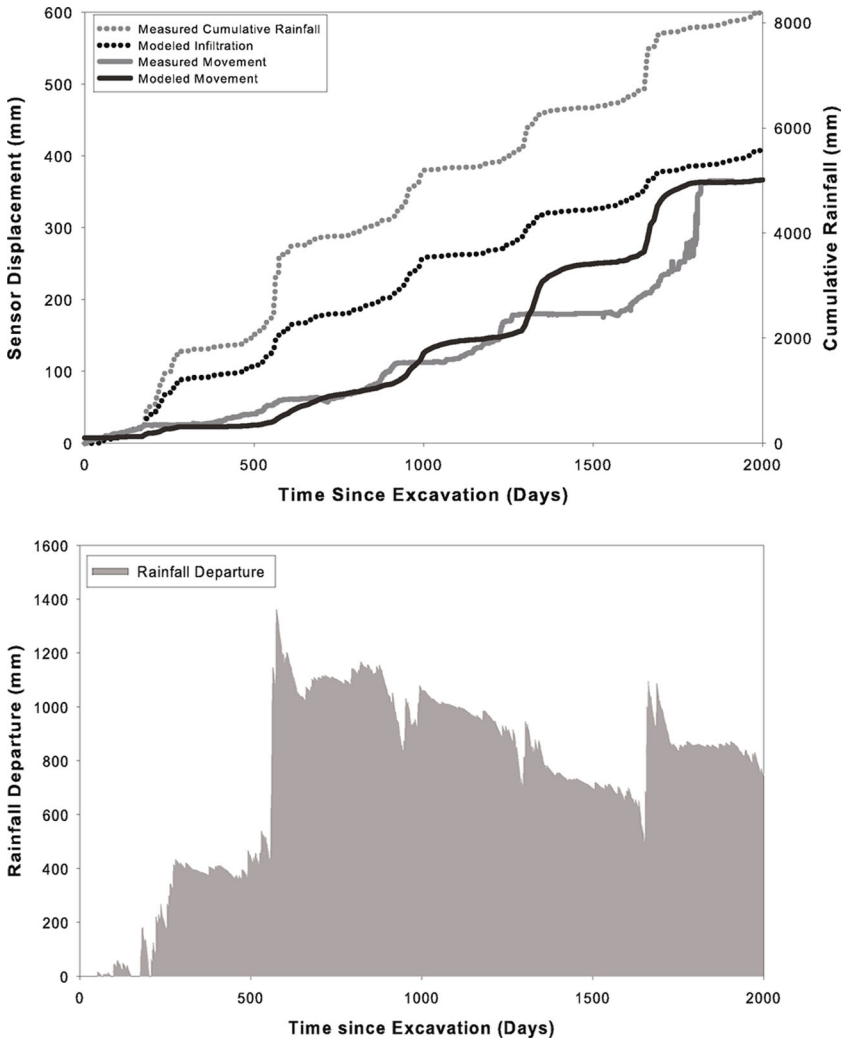

Fig. 7 **a** Measured/modeled slope movement and measured rainfall/modeled infiltration after excavation of toe. **b** Rainfall departure

controlling impact of the sustained above-average precipitation is demonstrated by gradual movement within the first 2 years (Fig. 7a) despite large, above-average rainfall events (Fig. 7b). However, larger seasonal displacements occurred after the rainy seasons in years 3 and 4, resulting in a very large movement (i.e., failure) in the fifth year after excavation. This phenomenon is also captured in the FE model, which captures a progressive rise in the sustained water table and a subsequent loss of suction within the slope. Figure 8 shows the simulated displacement, degree of saturation, and pore water pressure within time along three sections of the slope. The loss of suction facilitated soil shear, specifically at the interface between bedrock and at the toe of the slope near the excavation where the pressures from the sliding slope were large. The onset of these progressive movements was facilitated by large storm events at approximately 1600 and 2000 days after excavation that (1) diminished suction stresses, (2) decreased effective stress by increasing pore pressures from water table rise and seepage, and (3) increased driving forces by filling voids with the weight of water (Fig. 9). Ultimately, the slope was repaired using a concrete retaining wall after the large movements at the beginning of the sixth year and is currently stable.

As suction dissipated in the hillslope from sustained above-average rainfall, the kinematics of the slope failure changed with progressive movement. The initial movements and development of plasticity followed a translational failure mechanism that fits within an infinite slope failure mechanism (Lu and Godt 2008). The slope failure followed a translational mechanism on the upper slope, represented by relatively uniform displacements above the shear zone (Fig. 8). However, as failure progressed, rotational kinematics developed at the toe of the landslide, demonstrated by a non-uniform distribution of displacements, with maximum displacements occurring at the subsurface, implicative of rotation upwards. Figures 8 and 10 show incremental displacements of the slope with the given infiltration rates. As implied by displacements shown in Fig. 8, movement was mostly parallel to that of the bedrock for the beginning of the analysis, implicative of a translational, infinite slope failure. However, as the water table rose over time and suction stresses disappeared, the failure began to develop rotational kinematics at the toe (t=1440 days), and a secondary failure developed mid-slope (t=2160 days), likely corresponding to the next critical slope failure (Fig. 10). The shifting slope kinematics with progressive slope failures points

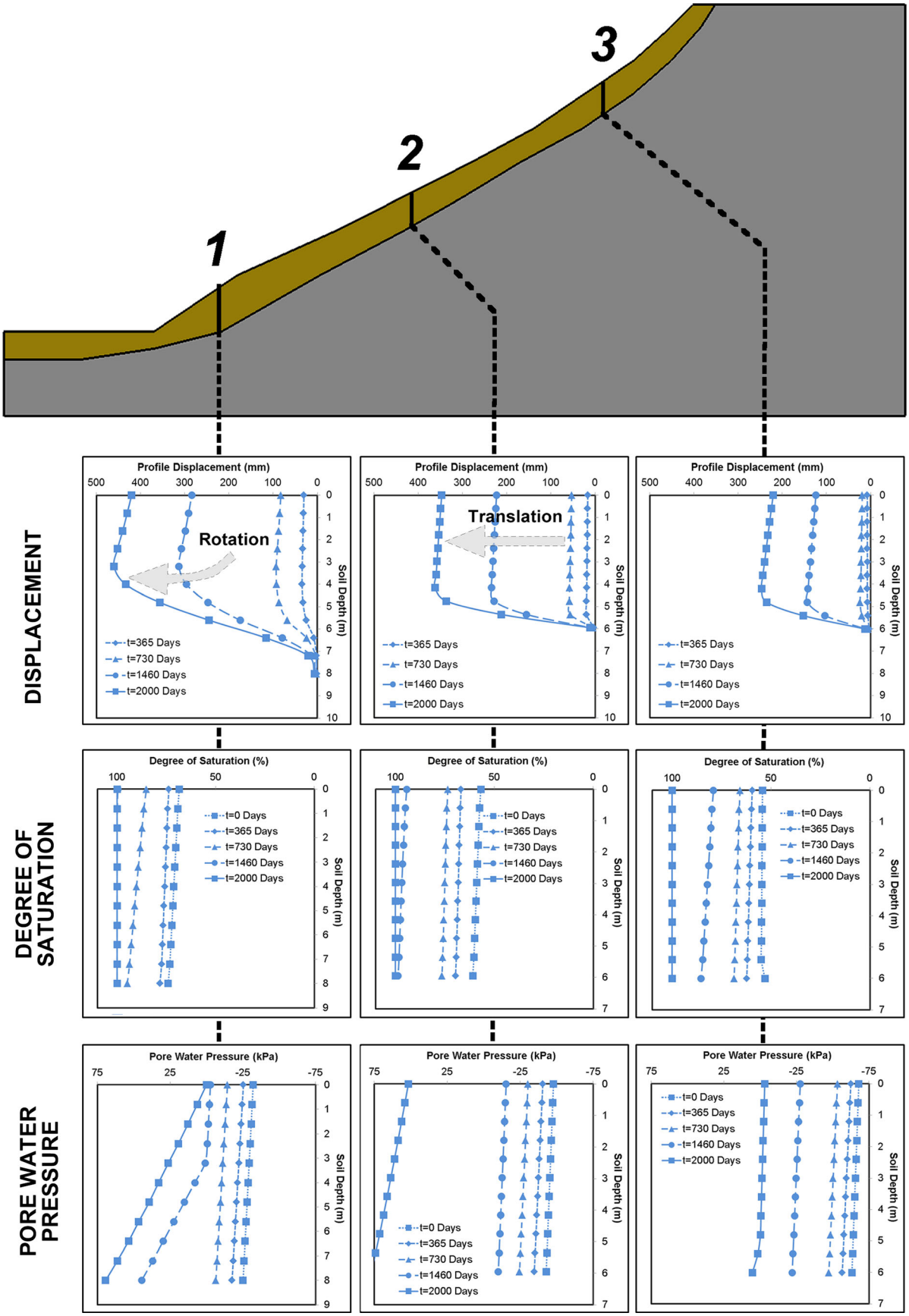

Fig. 8 Simulated displacement, degree of saturation and pore water pressure within time along three sections of the slope

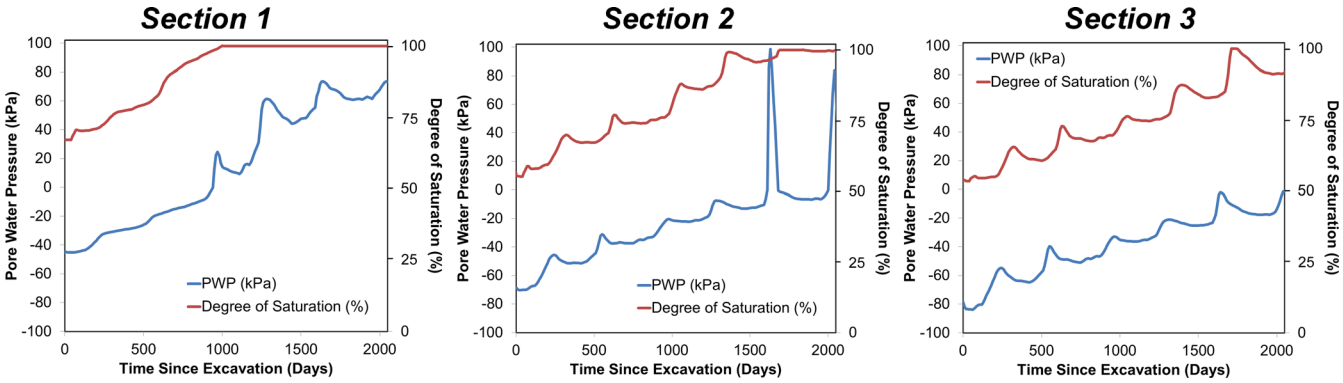

Fig. 9 Time history of pore water pressure and degree of saturation at the base of sections 1, 2, and 3

out constraints in simplified LE slope stability analyses—a critical failure surface is determined, but its subsequent stabilization and alternative destabilization of other slopes can be omitted with movement. However, use of tools that demonstrate the distribution of stability (e.g., factor of safety, plastic zones) may present critical and subcritical failure surfaces (Baker and Leshchinsky 2001) that are still relevant after initial destabilization of the critically weak failure surface. Use of tools that can capture the coupled pore pressure-stress-displacement response may provide more insight into the stabilizing behavior of slopes that are undergoing creep but also into the potentially non-intuitive effects of rainfall on progressive slope failures.

Conclusions

The presented case study described the progressive movement of a shallow landslide in Central South Korea after an excavation of the supporting toe and subsequent above-average rainfall. Measured soil data as well as real-time measurement of slope movement and precipitation enabled calibration of a numerical model based on FEM to capture the destabilization and associated of the slope. The numerical model employed Bishop's effective stress approach to quantify the effects of partial saturation on stabilizing suction stresses, as well as transient seepage analyses to introduce the non-uniform effects of actual rainfall data into the analysis. The resulting model provided insight into the complex behavior of a progressively failing slope. Conclusions from this case study include

- Numerical tools like FEM that allow for coupled stress-pore pressure-displacement analyses present a means of evaluating the progressive failure of slopes under rainfall. However, it can be difficult to capture the complex effects of vegetation and canopy cover, development of tension cracks, soil inhomogeneity, and erosion.
- Dependent on soil permeability and behavior under partially saturated conditions, sustained above-average rainfall may cause shallow landsliding when facilitated by changes in stability, like toe excavation.
- The kinematics of failing slopes may not always follow classical slope stability approaches (sliding block method, circular rotational failures, log-spiral, etc.) prior and during slope failure. Furthermore, the given kinematics of a slope failure may change with movement, redistribution of principal stresses, and dissipation of suction stress. Therefore, analyses like FE present a unique tool to evaluate the deformation behavior of failing slopes on a case-by-case basis.

The presented case study and associated FE analysis present the capability of advanced numerical tools in modeling the behavior of progressive slope failures on a case-by-case basis. However, this analysis comprises of constraints and requires assumptions that must be considered. First, assumption of two-dimensional conditions tend to be more conservative than reality when evaluating slope stability, but this analysis demonstrates that the concept can be applied to all FE methods, which can be two-dimensional or three-dimensional. Assumptions must be made about hydrology of the hillslope—specifically, the location (if any) of a permanent water table, anisotropy of the hydraulic properties of the overlying soil, fracture and hydraulics of bedrock, infiltration of precipitation, and formation of tension cracks. Finally, use of numerical tools like FE can be a time-consuming process requiring many input properties to perform an analysis—potentially challenging for model calibration, which can be a restrict application to study of individual slopes.

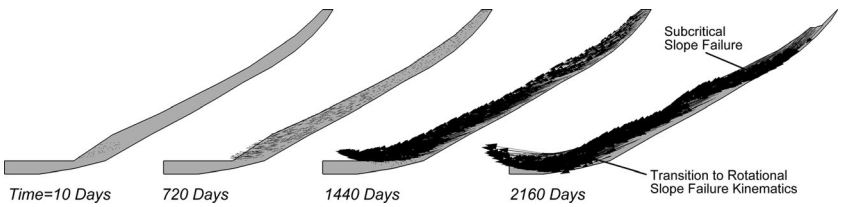

Fig. 10 Kinematics of slope movement over time as represented by incremental displacement vectors

Acknowledgments

The authors would like to thank Dr. Chungsik Yoo from Sungkyunkwan University, South Korea, for his thoughts and input regarding use of ABAQUS for analysis of partially saturated soils—it is greatly appreciated.

References

Baker R, Leshchinsky D (2001) Spatial distribution of safety factors. J Geotech Geoenviron 127(2):135–145

Bishop AW (1959) The principle of effective stress. Tek Ukeblad 106(39):859–863

Gardner WR (1958) Some steady state solutions of the unsaturated moisture flow equation with application to evaporation from a water table. Soil Sci 85(4):228–232

George RJ (1992) Hydraulic properties of groundwater systems in the saprolite and sediments of the wheatbelt, Western Australia. J Hydrol 130(1):251–278

Godt JW, Baum RL, Lu N (2009) Landsliding in partially saturated materials. Geophys Res Lett 36(2), L02403. doi:10.1029/2008GL035996

Hibbitt, Karlsson, Sorensen (2001) ABAQUS/standard user's Manual, 1. Hibbitt, Karlsson & Sorensen

Hsieh PA (1998) Scale effects in fluid flow through fractured geologic media. In: Garrison Sposito (ed) Scale dependence and scale invariance in hydrology. Cambridge: Cambridge University Press, p 335–353

Iverson RM, George DL, Allstadt K, Reid ME, Collins BD, Vallance JW, Schilling SP, Godt JW, Cannon CM, Magirl CS, Baum RL, Coe JA, Schulz WH, Bower JB (2015) Landslide mobility and hazards: implications of the 2014 Oso disaster. Earth Planet Sci Lett 412:197–208

Jiao JJ, Wang XS, Nandy S (2005) Confined groundwater zone and slope instability in weathered igneous rocks in Hong Kong. Eng Geol 80(1):71–92

Leshchinsky D (1997) Design procedure for geosynthetic reinforced steep slopes. Technical Report REMRGT-120 (temporary number), Waterways Experiment Station, U.S. Army Corps of Engineers, Vicksburg, Mississippi

Leshchinsky B (2013) Comparison of limit equilibrium and limit analysis for complex slopes. Proc GeoCongress, pp 1280-1289

Leshchinsky B, Ambauen S (2015) Limit equilibrium and limit analysis: comparison of benchmark slope stability problems. J Geotech Geoenviron Eng. doi:10.1061/(ASCE)GT.1943-5606.0001347

Leshchinsky D, Vahedifard F (2012) Impact of toe resistance in reinforced masonry block walls: design dilemma. J Geotech Geoenviron 138(2):236–240

Leung AK, Ng CWW (2013) Seasonal movement and groundwater flow mechanism in an unsaturated saprolitic hillslope. Landslides 10(4):455–467

Ling H, Ling HI (2012) Centrifuge model simulations of rainfall-induced slope instability. J Geotech Geoenviron 138(9):1151–1157

Ling HI, Wu MH, Leshchinsky D, Leshchinsky B (2009) Centrifuge modeling of slope instability. J Geotech Geoenviron Eng 135(6):758–767

Lu N, Godt J (2008) Infinite slope stability under steady unsaturated seepage conditions. Water Resour Res 44(11), W11404. doi:10.1029/2008WR006976

Lu N, Likos WJ (2004) Unsaturated soil mechanics. Wiley, New York

Lu N, Likos WJ (2006) Suction stress characteristic curve for unsaturated soil. J Geotech Geoenviron 132(2):131–142

Lu N, Şener B, Wayllace A, Godt JW (2012) Analysis of rainfall-induced slope instability using a field of local factor of safety. Water Resour Res 48(9), W09524. doi:10.1029/2012WR011830

Mencl V (1966) Mechanics of landslides with non-circular slip surfaces with special reference to the Vaiont slide. Geotechnique 16(4):329–337

Mualem Y (1976) A new model for predicting hydraulic conductivity of unsaturated porous media. Water Resour Res 12(3):513–522

Pagano L, Picarelli L, Rianna G, Urciuoli G (2010) A simple numerical procedure for timely prediction of precipitation-induced landslides in unsaturated pyroclastic soils. Landslides 7(3):273–289

Terzaghi K, Peck RB, Mesri G (1996) Soil mechanics in engineering practice. Wiley, New York

Tsai TL, Chen HE, Yang JC (2008) Numerical modeling of rainstorm-induced shallow landslides in saturated and unsaturated soils. Environ Geol 55(6):1269–1277

Vahedifard F, Leshchinsky B, Sehat S, Leshchinsky D (2014) Impact of cohesion on seismic design of geosynthetic-reinforced earth structures. J Geotech Geoenviron 140(6):04014016

Vahedifard F, Leshchinsky B, Mortezaei K, Lu N (2015a) Active earth pressures for unsaturated retaining structures. J Geotech Geoenviron Eng. doi: 10.1061/(ASCE)GT.1943-5606.0001356, 04015048

Vahedifard F, Leshchinsky D, Mortezaei K, Lu N (2015b) Effective stress-based limit equilibrium analysis for homogenous unsaturated slopes. Int J Geomech. doi:10.1061/(ASCE)GM.1943-5622.0000554

van Genuchten MT (1980) A closed form equation predicting the hydraulic conductivity of unsaturated soils. Soil Sci Soc Am 44:892–898

Wang JJ, Liang Y, Zhang HP, Wu Y, Lin X (2014) A loess landslide induced by excavation and rainfall. Landslides 11(1):141–152

Yoo C (2013) Effect of rainfall on performance of geosynthetic reinforced soil wall using stress-pore pressure coupled analysis. Geo-Congress 2013, pp. 566–573

Yoo C (2014) Effect of heavy rainfall on performance of geosynthetic reinforced wall. Proc. 10th International Conference on Geosynthetics, 10ICG Berlin, Germany, 21–25 September 2014

Yoo C, Jung H (2006) Case history of geosynthetic reinforced segmental retaining wall failure. J Geotech Geoenviron 132(12):1538–1548

B. Leshchinsky (✉)
Department of Forest Engineering, Resources and Management,
Oregon State University,
Corvallis, OR 97331, USA
e-mail: ben.leshchinsky@oregonstate.edu

F. Vahedifard
Department of Civil and Environmental Engineering,
Mississippi State University,
Mississippi State, MS 39762, USA

F. Vahedifard
e-mail: farshid@cee.msstate.edu

H.-. Koo · S.-. Kim
Geotechnical Engineering Research Division,
Korea Institute of Construction Technology,
Goyang City, South Korea
e-mail: hbkoo@kict.re.kr
e-mail: sshkim@kict.re.kr